

©2016, Elsevier. Licensed under the Creative Commons Attribution-NonCommercial-NoDerivatives

4.0 International <http://creativecommons.org/about/downloads>



Discovery of anti-cancer activity for benzo[1,2,4]triazin-7-ones: Very strong correlation to pleurotin and thioredoxin reductase inhibition

Martin Sweeney^{a, †}, Robert Coyle^{a, †}, Paul Kavanagh^a, Andrey A. Berezin^b, Daniele Lo Re^b, Georgia A. Zissimou^b, Panayiotis A. Koutentis^b, Michael P. Carty^{c,*} and Fawaz Aldabbagh^{a,*}

^a School of Chemistry, National University of Ireland Galway, University Road, Galway, Ireland

^b Department of Chemistry, University of Cyprus, P.O. Box 20537, 1678 Nicosia, Cyprus

^c Centre of Chromosome Biology, Biochemistry, School of Natural Sciences, National University of Ireland Galway, University Road, Galway, Ireland

† These authors contributed equally

ARTICLE INFO

ABSTRACT

Article history:

Received

Received in revised form

Accepted

Available online

Keywords:

Anti-tumor

Bioreduction

Heterocyclic compound

NCI-DTP COMPARE program

The thioredoxin (Trx)-thioredoxin reductase (TrxR) system plays a key role in maintaining the cellular redox balance with Trx being over-expressed in a number of cancers. Inhibition of TrxR is an important strategy for anti-cancer drug discovery. The natural product pleurotin is a well-known irreversible inhibitor of TrxR. The cytotoxicity data for benzo[1,2,4]triazin-7-ones showed very strong correlation (Pearson correlation coefficients ~ 0.8) to pleurotin using National Cancer Institute COMPARE analysis. A new 3-CF₃ substituted benzo[1,2,4]triazin-7-one gave submicromolar inhibition of TrxR, although the parent compound 1,3-diphenylbenzo[1,2,4]triazin-7-one was more cytotoxic against cancer cell lines. Benzo[1,2,4]triazin-7-ones exhibited different types of reversible inhibition of TrxR, and cyclic voltammetry showed characteristic quasi-reversible redox processes. Cell viability studies indicated strong dependence of cytotoxicity on substitution at the 6-position of the 1,3-diphenylbenzo[1,2,4]triazin-7-one ring.

1. Introduction

First identified in the late 1960s,¹ and isolated in 1980,² the rich chemistry of 1,3-diphenylbenzo[1,2,4]triazin-7-ones **1** (Figure 1) has more recently been explored.³⁻⁶ Benzotriazinone **1a** (R = H) and derivatives have been implicated as multi-target inhibitors in Alzheimer's disease of beta-amyloid (A β) aggregation and acetyl-(AChE)/butyryl- (BChE) cholinesterase.⁷ Scaffold **1** contains a highly conjugated iminoquinone motif and an iminoquinone derivative of imidazo[5,4-f]benzimidazoles was shown to have good specificity (Pearson correlation coefficient of 0.51) towards NAD(P)H:quinone oxidoreductase 1 (NQO1) expression using COMPARE analysis of toxicity towards the 60 cell lines at the National Cancer Institute (NCI) Development Therapeutics Program (DTP).⁸

We now report COMPARE analysis of the toxicity of benzotriazinones leading to the discovery of very strong correlations to pleurotin. The latter naturally occurring antibiotic is a *para*-quinone with a perhydroanthracene core, which was first isolated in the 1940s from the basidiomycete, *Pleurotus griseus*.⁹ Though pleurotin has been synthesized,¹⁰ a multi-gram fermentation process using *Hohenbuehelia atrocaerulea* for supply of pleurotin to the NCI has been reported.¹¹ Pleurotin possesses antibacterial,⁹ antifungal,¹² and anti-cancer activity, including inhibiting the hypoxia-induced factor (HIF-1 α), a transcription factor associated with many aspects of tumor growth.¹³ The underlying pathway to much of this biological

activity is pleurotin's ability to act as a potent inhibitor (IC₅₀ 0.17 μ M) of the thioredoxin (Trx)-thioredoxin reductase (TrxR) system.¹⁴

Earlier reports more specifically describe pleurotin as an irreversible inhibitor of TrxR with a K_i of 0.28 μ M.^{13,15} TrxR is a flavoprotein homodimer with each monomer containing a FAD prosthetic group, NADPH binding domain, and a redox-active selenothiol active site.^{16,17} TrxR is the only known enzyme to reduce Trx protein, which in turn provides reducing equivalents for a number of essential redox-dependent cellular processes, such as H₂O₂ metabolism, sulfate assimilation, and signal transduction.¹⁸ Trx protein is, however, over-expressed in a number of cancers, and is associated with increased cell proliferation, inhibition of apoptosis, and decreased patient survival.¹⁹ The reduced form of Trx protein inhibits the tumor suppressor protein PTEN (protein tyrosine phosphatase and tensin homolog).²⁰ Therefore negative regulation of Trx protein through TrxR inhibition is a significant strategy for the discovery of new anti-cancer agents. Herein, we investigate the structural requirements of the 1,3-diphenylbenzo[1,2,4]triazin-7-ones **1a-1l**, and the new compound 1-phenyl-3-(trifluoromethyl)benzo[1,2,4]triazin-7-one **2** for cytotoxicity against cancer cell lines, and inhibitory activity towards TrxR using a purified enzyme assay.

*Corresponding author. Tel.: +353 91 49 3120; fax: +353 91 49 5576

E-mail address: fawaz.aldabbagh@nuigalway.ie (F. Aldabbagh)

E-mail address: michael.carty@nuigalway.ie (M. P. Carty)

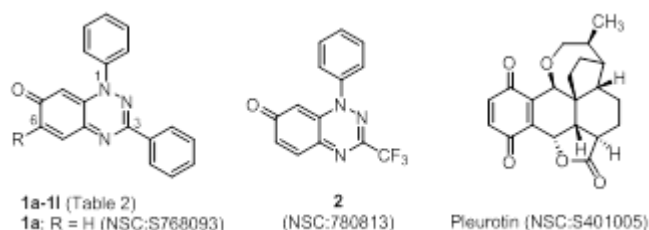
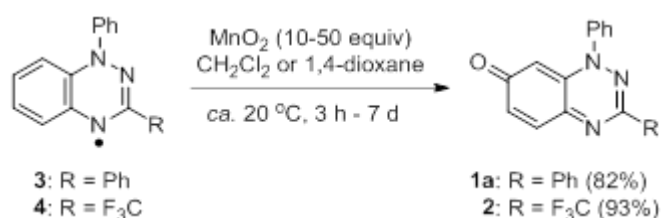


Figure 1. Benzo[1,2,4]triazin-7-ones **1a-1l**, **2** and pleurotin

2. Results and discussion

2.1. Synthesis

The synthesis of 1,3-diphenylbenzo[1,2,4]triazin-7-ones **1a-1l** was previously reported starting from 1,3-diphenylbenzo[1,2,4]triazin-4-yl radical **3**,⁵⁻⁶ and 1-phenyl-3-(trifluoro-methyl)benzo[1,2,4]triazin-7-one **2** is similarly accessible by mild MnO_2 oxidation of the analogous trifluoromethyl substituted radical **4** (Scheme 1).⁴



Scheme 1. Synthesis of benzo[1,2,4]triazin-7-ones

2.2. Development Therapeutic Program (DTP) National Cancer Institute (NCI) 60 human tumor cell line screen and COMPARE analysis

NCI one dose (10 μM) mean graph data of parent 1,3-diphenylbenzo[1,2,4]triazin-7-one **1a** showed strong growth inhibition against a number of cancer cell lines, particularly leukemia, colon, melanoma and renal cancers (Figure 2). Significant activity was apparent towards the prostate cancer line DU-145 and breast cancer cell line MCF-7, and these cell lines were available to us at our laboratory in Galway. We investigated the toxicity profile of **1a**, following selection of the compound for five-dose testing by the NCI, which established the GI_{50} , LC_{50} and TGI. The stated parameters provide the seed vector through which the NCI COMPARE algorithm determines closely matching cytotoxicity profiles.²¹ Complete single and five dose data for **1a** can be found in the supplementary data accompanying this article. COMPARE allows comparisons to be carried out towards all the synthetic compounds in the NCI database. The program applies the commercially available SAS statistical package to calculate a Pearson product-moment correlation coefficient (0 to ± 1) to establish the degree of similarity between two cytotoxicity profiles. Coefficients in the range (± 0.3 to ± 0.5) are considered medium strength, while those above (± 0.5) are considered strong. Out of ~70,000 compounds in the NCI database, pleurotin had one of the highest correlation coefficients to benzotriazinone **1a** at 0.84, which represents a very strong correlation (Table 1).

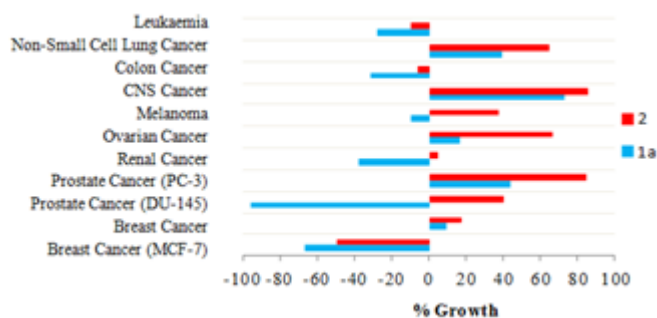


Figure 2. Summary of DTP NCI-60 single dose (10 μM) screening results for benzotriazinones **1a** and **2** expressed as average percent growth of each cancer cell type relative to untreated cells

1-Phenyl-3-(trifluoromethyl)benzo[1,2,4]triazin-7-one **2** is structurally distinct from benzotriazinones **1a-1l** since the 3-phenyl is replaced by a strong inductively electron-withdrawing trifluoromethyl (CF_3) group. Elevated toxicity towards the MCF-7 cell line supported trends in our later obtained MTT assay data (Table 2). Compound **2** appeared overall somewhat less cytotoxic against the main cancer types in comparison to **1a** (Figure 2), but with a very strong correlation to compound **1a** and pleurotin using COMPARE analysis after the five dose testing (Table 1). The large Pearson correlation coefficients (~ 0.8) indicated possible common pathways for anti-cancer activity.

Table 1. Pearson correlation coefficients obtained by COMPARE analysis

Compound	Pleurotin	2
1a	0.842	0.803
2	0.793	-

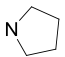
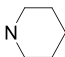
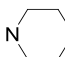
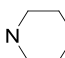
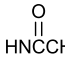
2.3. Cytotoxicity against normal and cancer cell lines using the MTT assay

To determine the specificity and overall cytotoxicity towards selected cancer cell lines, the effect of substitution at the 6-position of the 1,3-diphenylbenzo[1,2,4]triazin-7-one scaffold with amine, amide and alkoxy substituents was investigated (compounds **1a-1l** in Figure 1). Cytotoxicity was determined against the prostate cancer cell line DU-145 and the breast cancer cell line MCF-7 using the MTT assay (Table 2). These cell lines form part of the NCI-60 human tumor cell line screen. As a control the response of a normal human-skin fibroblast cell line GM00637 was determined.

Pleurotin displayed submicromolar toxicity towards all three cell lines investigated, with parent **1a** showing comparable toxicity. Substitution with methoxy- and ethoxy-groups in compounds **1k** and **1l** and amide in **1j** decreased toxicity to negligible values. The methoxy substituent (OMe) on heterocyclic quinones has been shown to lead to significant reductions in toxicity towards cell lines in comparison to its replacement with an aziridiny substituent. The trends in toxicity correlate to a reduced electron-affinity property as a result of the electron donation by the alkoxy substituent.^{22,23} Cyclic amine substituents in **1f-1i** led to a general reduction in toxicity values compared to the parent **1a**, with the exception of pyrrolo-substituted benzotriazinone **1f**. Compound

1f showed the greatest specificity toward the MCF-7 cell line similar to the toxicity of pleurotin. Among the acyclic amines **1b-1e**, secondary amine substituents in **1c** and **1d** gave submicromolar toxicity. The ethylamino-substituent in **1d** has a similar potency to the parent **1a** with a comparative approximate two-fold reduction in toxicity towards the MCF-7 cell line. 1-Phenyl-3-(trifluoromethyl)benzo[1,2,4]triazin-7-one **2** with a strong electron-withdrawing substituent at the 3-position was evaluated due to the lack of availability of benzotriazinones with electron-withdrawing substituents at the 6-position. Compound **2** showed submicromolar toxicity towards the two cancer cell lines (DU-145 and MCF-7) with a 2- to 3-fold decrease in toxicity towards the normal skin fibroblast cell line (GM00637).

Table 2. Cytotoxicity evaluation using the MTT assay: IC₅₀ values (μM)^a

Compd	R	Cell Lines		
		GM00637	DU-145	MCF-7
Pleurotin		0.51 ± 0.12	0.43 ± 0.06	0.28 ± 0.03
1a	H	0.23 ± 0.01	0.23 ± 0.03	0.81 ± 0.08
1b	NH ₂	2.04 ± 0.21	1.83 ± 0.08	0.95 ± 0.03
1c	NHMe	0.93 ± 0.03	0.98 ± 0.06	0.69 ± 0.12
1d	NHEt	0.24 ± 0.01	0.22 ± 0.01	1.62 ± 0.24
1e	NEt ₂	2.73 ± 0.36	3.11 ± 0.08	>5.0
1f		1.79 ± 0.12	2.46 ± 0.19	0.36 ± 0.08
1g		1.19 ± 0.02	0.61 ± 0.05	1.98 ± 0.06
1h		2.29 ± 0.06	3.21 ± 0.37	2.37 ± 0.07
1i		1.63 ± 0.31	1.22 ± 0.06	0.97 ± 0.16
1j		>5.0	>5.0	>5.0
1k	OMe	>5.0	>5.0	>5.0
1l	OEt	>5.0	>5.0	>5.0
2		1.61 ± 0.21	0.85 ± 0.04	0.60 ± 0.13

^a IC₅₀ represents the compound concentration required for the reduction of the mean cell viability to 50% of the control value after incubation for 72 h at 37 °C

2.4. Cyclic voltammetry

Cyclic voltammetry on compounds **1a** and **2** were carried out in anticipation that bioreductive activation may be implicated in cytotoxicity (Figure 3). Redox response experiments were carried out in dichloromethane, which showed that both **1a** and **2** undergo two characteristic quasi-reversible one-electron redox processes corresponding to the 0/-1 redox transition (I and I') and -1/-2 redox transition (II and II'). Benzotriazinone **1a** displayed a redox potential (E°) of -1.12 V vs. Fc/Fc⁺ for the 0/-1 redox transition (I) and -1.75 V vs. Fc/Fc⁺ for the -1/-2 redox transition (II). Benzotriazinone **2** produced a similar redox response to **1a**, although E° values for equivalent redox couples (I' and II') are

shifted by approximately +0.23 V in the positive direction. This can be attributed to the strong inductive withdrawal by the 3-CF₃ of **2** relative to the 3-phenyl substituent present in **1a** resulting in an enhanced susceptibility of **2** to undergo reduction.

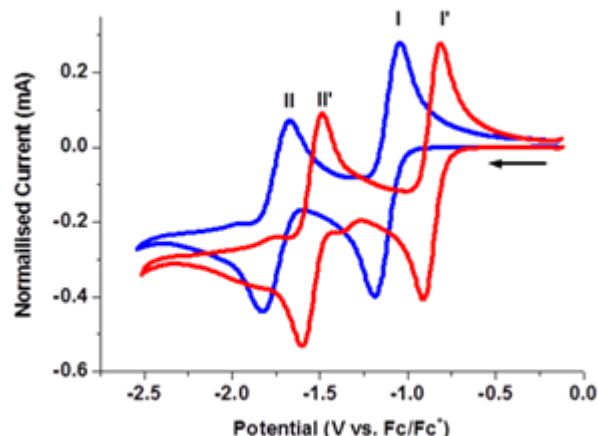


Figure 3. Cyclic voltammograms of **1a** (blue line) and **2** (red line) recorded in dichloromethane (0.1 M TBAP) at a glassy carbon electrode (scan rate: 0.1 V s⁻¹). Arrow indicates direction of scan

Table 3. Formal Potentials (E°) (±0.010 V) calculated as (E_{pc} + E_{pa})/2 from cyclic voltammograms recorded at 100 mV s⁻¹

Compound	E° [V] versus Fc/Fc ⁺	
	E° (I)	E° (II)
1a	-1.12	-1.75
2	-0.86	-1.55

2.5. Thioredoxin reductase (TrxR) inhibition assays

To determine whether **1a** and **2** inhibited TrxR, and to identify the mode of inhibition, enzyme activity was estimated in the absence or presence of varying concentrations of inhibitor. Data was analysed using the Lineweaver-Burk plot (Figure 4). In the case of **1a** V_{max} decreased and K_m increased with increasing inhibitor, characteristic of mixed inhibition. However, **2** is more characteristic of uncompetitive inhibition where V_{max} decreased with increasing inhibitor and K_m was lower in the presence of inhibitor, than in the uninhibited condition.

To estimate the K_i value, a secondary plot (Figure 5) of the slopes of the Lineweaver-Burk plot against inhibitor concentrations was generated. K_i values were found to be 3.90 and 0.78 μM for compounds **1a** and **2**, respectively. The lower K_i for **2** towards the reductase enzyme may be attributed to it being more reducible than **1a** as determined by cyclic voltammetry (Figure 3). Therefore benzotriazinones **1a** and **2** clearly inhibit TrxR, but unlike pleurotin the mode of inhibition is reversible rather than irreversible. The K_i value for the electron-deficient iminoquinone **2** is closer in magnitude to that of pleurotin (K_i 0.28 μM).^{13,15}

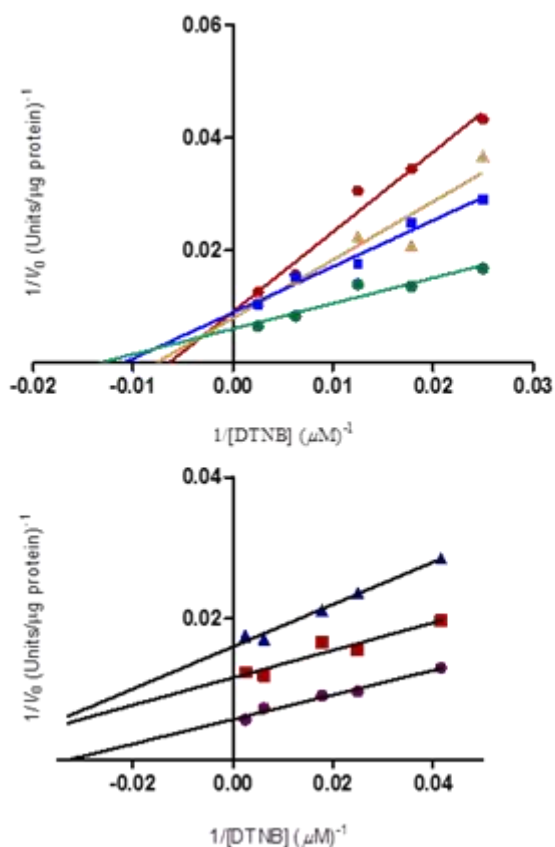


Figure 4. Kinetics of thioredoxin reductase (TrxR) inhibition by 1,3-diphenylbenzo[1,2,4]-triazin-7-one **1a** and 1-phenyl-3-(trifluoromethyl)benzo[1,2,4]triazin-7-one **2** using 5,5'-dithiobis(2-nitrobenzoic) acid (DTNB) as the substrate: (a) Lineweaver-Burk plot with inhibitor **1a** concentrations of 0 (—●—), 0.15 (—■—), 0.30 (—▲—) and 0.50 (—◆—) μM . (b) Lineweaver-Burk plot with inhibitor **2** concentrations of 0 (—●—), 0.30 (—■—) and 1 (—▲—) μM

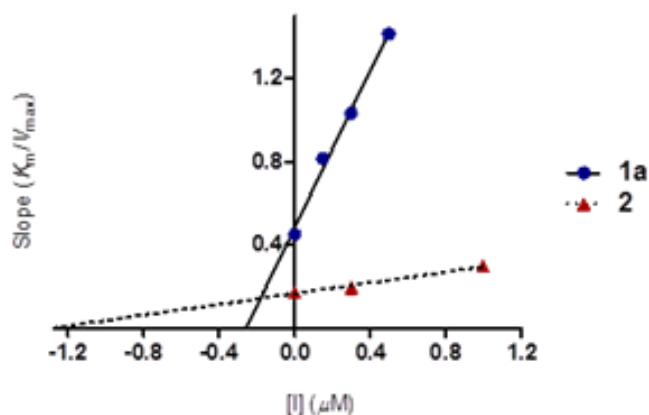


Figure 5. Graphical determination of K_i for 1,3-diphenylbenzo[1,2,4]triazin-7-one **1a** and 1-phenyl-3-(trifluoromethyl)benzo[1,2,4]triazin-7-one **2** using the slopes of the Lineweaver-Burk plots in Figure 4 versus inhibitor concentrations.

3. Conclusions

Using NCI COMPARE program, parent benzotriazinone **1a** and 3- CF_3 substituted analogue **2** were found to have very strong correlations to a naturally occurring anti-cancer agent pleurotin. Benzotriazinones **1a** and **2** are TrxR inhibitors, although the mechanism for inhibition is reversible rather than irreversible as

for pleurotin. The latter may be attributed to differences in chemical structure with pleurotin containing an isolated non-conjugated quinone motif.

Varying the substituent at the 6-position of the 1,3-diphenylbenzo[1,2,4]triazin-7-ones has a profound effect on toxicity. Benzotriazinone **1a** is generally more cytotoxic towards cancer cell lines, although compound **2** shows greater specificity towards solid tumor cell lines in comparison to a normal fibroblast cell line. The latter CF_3 -substituted compound is more easily reducible and shows a more than five-fold greater inhibition of TrxR. Differences in the extent and type of TrxR inhibition as well as other cellular interactions may modulate the cytotoxicity of **1a** and **2** towards normal and cancer cell lines.

4. Experimental section

4.1. Synthetic materials and methods

4.1.1. General

1,4-Dioxane was dried over CaH_2 . Reactions were protected from atmospheric moisture by CaCl_2 drying tubes. All volatiles were removed under reduced pressure. All reaction mixtures and column eluents were monitored by TLC using commercial glass backed thin layer chromatography (TLC) plates (Merck Kieselgel 60 F₂₅₄). The plates were observed under UV light at 254 and 365 nm. The technique of dry flash chromatography was used throughout for all non-TLC scale chromatographic separations using Merck Silica Gel 60 (less than 0.063 mm).²⁴ Melting and decomposition points were determined using a TA Instruments DSC Q1000 with samples hermetically sealed in aluminium pans under an argon atmosphere using heating rates of 5 $^\circ\text{C}/\text{min}$. IR spectra were recorded on a Shimadzu FTIR-NIR Prestige-21 spectrometer with a Pike Miracle Ge ATR accessory and strong, medium and weak peaks are represented by s, m and w, respectively. ^1H and ^{13}C NMR spectra were recorded on a BrukerAvance 300 machine (at 300 and 75 MHz, respectively). Deuterated solvents were used for homonuclear lock and the signals are referenced to the deuterated solvent peaks. MALDI-TOF MS were conducted on a Bruker BIFLEX III time-of-flight (TOF) mass spectrometer. 1,3-Diphenylbenzo[1,2,4]triazin-7-one (**1a**),³ 6-amino-1,3-diphenylbenzo[1,2,4]triazin-7-one (**1b**),⁶ 6-(methylamino)-1,3-diphenylbenzo[1,2,4]triazin-7-one (**1c**),⁵ 6-(ethylamino)-1,3-diphenylbenzo[1,2,4]triazin-7-one (**1d**),⁶ 6-(diethylamino)-1,3-diphenylbenzo[1,2,4]triazin-7-one (**1e**),⁷ 1,3-diphenyl-6-(pyrrolidin-1-yl)benzo[1,2,4]triazin-7-one (**1f**),⁷ 1,3-diphenyl-6-(piperidin-1-yl)benzo[1,2,4]triazin-7-one (**1g**),⁶ 6-morpholino-1,3-diphenylbenzo[1,2,4]triazin-7-one (**1h**),⁷ 1,3-diphenyl-6-thiomorpholinobenzo[1,2,4]triazin-7-one (**1i**),⁷ *N*-(7-oxo-1,3-diphenyl-1,7-dihydrobenzo[1,2,4]triazin-6-yl)acetamide (**1j**),⁵ 6-methoxy-1,3-diphenylbenzo[1,2,4]triazin-7-one (**1k**),⁷ and 6-ethoxy-1,3-diphenylbenzo[1,2,4]triazin-7-one (**1l**)⁶ were synthesized according to literature procedures.

4.1.2. 1-Phenyl-3-(trifluoromethyl)benzo[1,2,4]triazin-7-one (**2**)

To a stirred solution of 1-phenyl-3-(trifluoromethyl)-1,4-dihydro-1,2,4-benzotriazin-4-yl (**4**)⁴ (44.2 mg, 0.16 mmol) in dry 1,4-dioxane (4 mL) at ca. 20 $^\circ\text{C}$ was added MnO_2 (0.696 g, 50 equiv) and the reaction mixture stirred vigorously for 3 h. Upon completion, the reaction was poured onto a short silica pad and washed with *n*-hexane. Chromatography (*n*-hexane/diethyl ether, 1:1) afforded the *title compound* **2** as dark purple shiny needles (43.3 mg, 93%); mp (DSC) onset: 140.5 $^\circ\text{C}$, peak max: 144.9 $^\circ\text{C}$ (from *n*-hexane); R_f 0.58 (*t*-BuOMe); (found: C, 57.65; H, 2.67; N, 14.35. $\text{C}_{14}\text{H}_8\text{F}_3\text{N}_3\text{O}$ requires C, 57.74; H, 2.77; N, 14.43%);

λ_{\max} (DCM)/nm 281 (log ϵ 3.36), 291 inf (3.25), 481 inf (2.40), 528 (2.56), 561 (2.48), 607 inf (2.12); ν_{\max} /cm⁻¹ 3061w (Ar C-H), 1620m, 1605m, 1597m, 1549s (C=O), 1495m, 1466w, 1458w, 1422w, 1400s, 1356s, 1333m, 1319w, 1304w, 1294w, 1246w, 1217s, 1200s, 1177m, 1150s, 1136s, 1113m, 1096s, 1074w, 1030w, 1001w, 984m, 926w, 908w, 853s, 824m, 775m, 733w; δ_{H} (300 MHz, CDCl₃) 7.72 (1H, d, *J* 9.8 Hz), 7.67-7.58 (3H, m), 7.56-7.48 (2H, m), 7.33 (1H, dd, *J* 9.8, 2.1 Hz), 6.12 (1H, d, *J* 1.9 Hz); δ_{C} (75 MHz, CDCl₃) 182.6 (s), 156.3 (s), 143.1 (d), 142.4 (q, ²*J*_{FC} 39.0 Hz, CCF₃), 139.9 (s), 136.6 (s), 132.2 (d), 130.8 (d), 130.3 (d), 125.2 (d), 119.2 (q, ¹*J*_{FC} 273.6 Hz, CF₃), 100.0 (d); MALDI-TOF (*m/z*): 293 (MH⁺+1, 4%), 292 (MH⁺, 100), 264 (7), 257 (70), 239 (1), 209 (6), 196 (2), 172 (1), 133 (3).

4.2. Cell culture and cytotoxicity evaluation

4.2.1. Cell culture

An SV40-transformed normal human fibroblast cell line (repository number GM00637) was obtained from the National Institute for General Medical Sciences (NIGMS) Human Genetic Cell Repository (Coriell Institute for Medical Research, New Jersey, USA). The DU-145 prostate cancer cell line (ATCC repository number HTB-81) was obtained from Prof. R.W.G. Watson, School of Medicine & Medical Sciences, University College Dublin, Ireland. The MCF-7 cell line, a human breast cancer cell line was obtained from Dr. Adrienne Gorman, Biochemistry, School of Natural Sciences, National University of Ireland Galway.

The SV40-transformed normal human skin fibroblast cell line (GM00637) was grown in minimum essential media (MEM) Eagle-Earle BSS supplemented with 15% heat-inactivated fetal bovine serum (FBS), penicillin-streptomycin, 2 mM L-glutamine, 2X essential and non-essential amino acids and vitamins. DU-145 prostate cancer cells were grown in RPMI-1640 medium supplemented with 10% heat-inactivated fetal bovine serum, penicillin-streptomycin and 2 mM L-glutamine. MCF-7 cells were cultured in Dulbecco's modified Eagle's medium (DMEM) containing high glucose (4.5 mg/mL) and supplemented with 10% heat-inactivated FBS and 1% penicillin-streptomycin.

4.2.2. Cytotoxicity measurement

Cell viability was determined using the MTT colorimetric assay.²⁵ Normal cells were plated into 96-well plates at a density of 10,000 cells per well (200 μ L per well) and allowed to adhere over a period of 24 h. DU-145 cells were plated into 96-well plates at a density of 2,000 cells per well (200 μ L per well) and allowed to adhere over a period of 24 h. MCF-7 cells were plated into 96-well plates at a density of 1,000 cells per well (200 μ L per well) and allowed to adhere over a period of 24 h. Compound solutions were applied in DMSO (1% v/v final concentration in well). Cells were then incubated at 37 °C under a humidified atmosphere containing 5% CO₂ for 72 h. Control cells were exposed to an equivalent concentration of DMSO alone. MTT (20 μ L, 5 mg/mL solution) was added, and the cells were incubated for another 4 h. The supernatant was removed carefully by pipette. The resultant MTT formazan crystals were dissolved in 100 μ L of DMSO and absorbance was determined on a plate reader at 550 nm with a reference at 690 nm. Cell viability is expressed as a percentage of the DMSO-only treated value. Dose response curves were analyzed by non-linear regression analysis and IC₅₀ values were estimated using GraphPad Prism software, v 6.03 (GraphPad Inc., San Diego, CA, USA).

4.3. Electrochemistry

Cyclic voltammograms were recorded using a Palmsens EmStat3+ potentiostat. Samples (~2 mmol) were dissolved in

dichloromethane containing 0.1 M tetrabutylammonium perchlorate (TBAP) as supporting electrolyte and 1 mM ferrocene (Fc) as an internal reference. Voltammograms were recorded in a single compartment electrochemical cell (0.5 mL volume) containing a glassy carbon disk working electrode (3 mm diameter), an Ag/AgCl reference electrode and a Pt wire counter electrode. All measurements were recorded under nitrogen at room temperature.

4.4. Thioredoxin reductase (TrxR) inhibition studies

4.4.1. Materials

The thioredoxin reductase assay kit (Sigma Aldrich) contained all reagents and enzyme required for the thioredoxin reductase assay and was used as received. Rat liver thioredoxin reductase was in 50 mM Tris-HCl, pH 7.4, containing 1 mM EDTA, 300 mM NaCl, and 10% glycerol. The working buffer contained 100 mM potassium phosphate with 10 mM EDTA, 0.24 mM NADPH and the assay buffer 5 \times contained 500 mM potassium phosphate, pH 7.0 and 50 mM EDTA.

4.4.2. Enzyme kinetics

The kinetics of rat liver thioredoxin reductase (TrxR) inhibition was analysed in 96-well microtiter plates. The experimental setup follows manufacturer's instructions. The reduction of 5,5'-dithiobis(2-nitrobenzoic) acid (DTNB) with NADPH to 5-thio-2-nitro-benzoic acid (TNB) gave a linear increase in absorbance at 405 nm and 27 °C. Each assay point represents an average from three independent experiments carried out in duplicate. The absorbance was measured at intervals of 5 minutes for a period of 50 minutes. Absorbance was measured using a Biotek Powerwave XS2 plate reader. Taking ΔA_{405} from the linear portion of the absorbance plot, TrxR activity was quantified using equation 1.

$$\text{Unit mL}^{-1} = \frac{\Delta A_{405} \text{ min}^{-1} (\text{thioredoxin reductase}) \times \text{dil} \times \text{vol}}{\text{enzvol}}$$

Equation 1

A *unit* of mammalian TrxR is the amount of enzyme that will cause an increase in A_{405} of 1.0 min⁻¹mL⁻¹ at pH 7.0 and 25 °C, where $\Delta A_{405} \text{ min}^{-1}(\text{TrxR}) = [\Delta A_{405} \text{ min}^{-1}(\text{sample}) - \Delta A_{405} \text{ min}^{-1}(\text{sample} + \text{inhibitor})]$; dil = sample dilution factor; vol = total reaction volume; enzvol = enzyme volume.

The enzyme specific activity (Units/ μ g protein) or initial velocity (V_0) is calculated by dividing the UnitmL⁻¹ by TrxR concentration (2.5 \times 10⁻³ μ g/mL) in the well. The double reciprocal Lineweaver-Burk is plotted using GraphPad Prism software, v 6.03 (GraphPad Inc., San Diego, CA, USA). The final concentration of DMSO in the assay did not exceed 3.2% (v/v).

Acknowledgements

FA thanks the Irish Research Council (IRC) for a Government of Ireland Postgraduate Scholarship for Martin Sweeney and College of Science, National University of Ireland Galway (NUI Galway) for a postgraduate scholarship for Robert Coyle. We thank the National Cancer Institute (USA), Development Therapeutic Program for providing us with a small quantity of pleurotin. PAK thanks the Cyprus Research Promotion Foundation [Grants: NEAYPODOMH/NEKYP/0308/02 and YGEIA/BIOS/0308(BIE)/13], the University of Cyprus (Medium Sized Grant), and the following organizations in Cyprus for generous donations of chemicals and glassware: the State General Laboratory, the Agricultural Research Institute, the Ministry of Agriculture, Medochemie Ltd and Biotronics Ltd. Furthermore,

PAK thanks the A. G. Leventis Foundation for helping to establish the NMR facility in the University of Cyprus.

Supplementary data

Supplementary data includes ^1H and ^{13}C NMR spectra of compound **2**, cell viability plots and NCI COMPARE analysis.

References and notes

1. Huisgen, R.; Wulff, J. *Chem Ber.* **1969**, *102*, 1848. DOI: [10.1002/cber.19691020609](https://doi.org/10.1002/cber.19691020609)
2. Neugebauer, F. A.; Umminger, I. *Chem Ber.* **1980**, *113*, 1205. DOI: [10.1002/cber.19801130402](https://doi.org/10.1002/cber.19801130402)
3. Koutentis, P. A.; Lo Re, D. *Synthesis* **2010**, 2075. DOI: [10.1055/s-0029-1218782](https://doi.org/10.1055/s-0029-1218782)
4. Constantinides, C. P.; Berezin, A. A.; Zissimou, G. A.; Manoli, M.; Leitus, G. M.; Bendikov, M.; Probert, M. R.; Rawson, J. M.; Koutentis, P. A. *J. Am. Chem. Soc.* **2014**, *136*, 11906. DOI: [10.1021/ja5063746](https://doi.org/10.1021/ja5063746)
5. Berezin, A. A.; Constantinides, C. P.; Drouza, C.; Manoli, M.; Koutentis, P. A. *Org. Lett.* **2012**, *14*, 5586. DOI: [10.1021/ol302714j](https://doi.org/10.1021/ol302714j)
6. Koutentis, P. A.; Krassos, H.; Lo Re, D. *Org. Biomol Chem.* **2011**, *9*, 5228. DOI: [10.1039/C1OB05410D](https://doi.org/10.1039/C1OB05410D)
7. Catto, M.; Berezin, A. A.; Lo Re, D.; Loizou, G.; Demetriades, M.; De Stradis, A.; Campagna, F.; Koutentis, P. A.; Carotti, A. *Eur. J. Med. Chem.* **2012**, *58*, 84. DOI: [10.1016/j.ejmech.2012.10.003](https://doi.org/10.1016/j.ejmech.2012.10.003)
8. Fagan, V.; Bonham, S.; Carty, M. P.; Saenz-Méndez, P.; Eriksson, L. A.; Aldabbagh, F. *Bioorg. Med. Chem.* **2012**, *20*, 3223. DOI: [10.1016/j.bmc.2012.03.063](https://doi.org/10.1016/j.bmc.2012.03.063)
9. Robbins, W. J.; Kavanagh, F.; Hervey, A. *Proc. Natl. Acad. Sci.* **1947**, *33*, 171. DOI: [10.1073/pnas.33.6.171](https://doi.org/10.1073/pnas.33.6.171)
10. Hart, D. J.; Huang, H. C.; Krishnamurthy, R.; Schwartz, T. *J. Am. Chem. Soc.* **1989**, *111*, 7507. DOI: [10.1021/ja00201a035](https://doi.org/10.1021/ja00201a035)
11. Shipley, S. M.; Barr, A. L.; Graf, S. J.; Collins, R. P.; McCloud, T. G.; Newman, D. J. *J. Ind. Microbiol. Biotechnol.* **2006**, *33*, 463. DOI: [10.1007/s10295-006-0089-0](https://doi.org/10.1007/s10295-006-0089-0)
12. Berdicevsky, I.; Kaufman, G.; Newman, D. J.; Horwitz, B. A. *Mycoses* **2009**, *52*, 313. DOI: [10.1111/j.1439-0507.2008.01620.x](https://doi.org/10.1111/j.1439-0507.2008.01620.x)
13. Welsh, S. J.; Williams, R. R.; Birmingham, A.; Newman, D. J.; Kirkpatrick, D. L.; Powis, G. *Mol. Cancer Ther.* **2003**, *2*, 235.
14. Wipf, P.; Hopkins, T. D.; Jung, J. -K.; Rodriguez, S.; Birmingham, A.; Southwick, E. C.; Lazo, J. S.; Powis, G. *Bioorg. Med. Chem. Lett.* **2001**, *11*, 2637. DOI: [10.1016/S0960-894X\(01\)00525-X](https://doi.org/10.1016/S0960-894X(01)00525-X)
15. Kunkel, M. W.; Kirkpatrick, D. L.; Johnson, J. L.; Powis, G. *Anti-Cancer Drug Des.* **1997**, *12*, 659.
16. Gromer, S.; Arscott, L. D.; Williams Jr, C. H.; Schirmer, R. H.; Becker, K. *J. Biol. Chem.* **1998**, *273*, 20096. DOI: [10.1074/jbc.273.32.20096](https://doi.org/10.1074/jbc.273.32.20096)
17. Mustacich, D.; Powis, G. *Biochem. J.* **2000**, *346*, 1. DOI: [10.1042/bj3460001](https://doi.org/10.1042/bj3460001)
18. Arnér, E. S. J.; Holmgren, A. *Eur. J. Biochem.* **2000**, *267*, 6102. DOI: [10.1046/j.1432-1327.2000.01701.x](https://doi.org/10.1046/j.1432-1327.2000.01701.x)
19. Cha, M.-K.; Suh, K.-H.; Kim, I.-H. *J. Exp. Clin. Oncol.* **2009**, *28*, 93. DOI: [10.1186/1756-9966-28-93](https://doi.org/10.1186/1756-9966-28-93)
20. Meuillet, E. J.; Mahadevan, D.; Berggren, M.; Coon, A.; Powis, G. *Arch Biochem. Biophys.* **2004**, *429*, 123. DOI: [10.1016/j.abb.2004.04.020](https://doi.org/10.1016/j.abb.2004.04.020)
21. Shoemaker, R. H. *Nature Rev. Cancer* **2006**, *6*, 813. DOI: [10.1038/nrc1951](https://doi.org/10.1038/nrc1951)
22. Naylor, M. A.; Jaffar, M.; Nolan, J.; Stephens, M. A.; Butler, S.; Patel, K. B.; Everett, S. A.; Adams, G. E.; Stratford, I. J. *J. Med. Chem.* **1997**, *40*, 2335. DOI: [10.1021/jm9608422](https://doi.org/10.1021/jm9608422)
23. Fahey, K.; O'Donovan, L.; Carr, M.; Carty, M. P.; Aldabbagh, F. *Eur. J. Med. Chem.*, **2010**, *45*, 1873. DOI: [10.1016/j.ejmech.2010.01.026](https://doi.org/10.1016/j.ejmech.2010.01.026)
24. Harwood, L. M. *Aldrichimica Acta* **1985**, *18*, 25.
25. Mosmann, T. *J. Immunol. Methods.* **1983**, *65*, 55. DOI: [10.1016/0022-1759\(83\)90303-4](https://doi.org/10.1016/0022-1759(83)90303-4)